

1 Detection of foray behaviour in the zooplankton of the Antarctic Polar  
2 Front region

3

4 Victoria Dewar-Fowler<sub>1</sub>, Carol Robinson<sub>2</sub>, Ryan A. Saunders<sub>1</sub>, Geraint A. Tarling<sub>1</sub>\*

5

6 1. British Antarctic Survey, High Cross, Madingley Rd, Cambridge, CB3 0ET, UK

7 2. School of Environmental Sciences, University of East Anglia, Norwich, NR4 7TJ, UK

8 \* corresponding author

9

10 **Abstract**

11 In addition to diel vertical migration, individual zooplankton may also make a number of shorter-  
12 term migrations, or forays, into the surface layers from deeper depths. Direct observation of these  
13 forays is limited, particularly in the open ocean, which hinders our understanding of carbon flux via  
14 the Biological Carbon Pump (BCP). We designed a novel net device capable of trapping zooplankton  
15 during such forays. The Motion compensated Upward and Downward Looking (MUDL) net device  
16 consisted of two conical nets, one looking upwards and the other looking downwards, designed for  
17 stationary deployment at a set depth, into which migrating individuals must swim in order to be  
18 captured. The device was deployed at different time points within the diel cycle and at contrasting  
19 environments across Antarctic Polar Front region in the southwest Atlantic sector of the Southern  
20 Ocean. A range of zooplankton species were captured, with differences in abundance and species  
21 composition between times of day, net direction and sites. Of particular note was the large  
22 contribution of the copepod *Oithona* spp. to catches of both the upward and downward looking  
23 nets. Our study demonstrates the utility of our MUDL net for future ecosystem studies in the open  
24 ocean, particularly in relation to quantifying vertical carbon flux via the BCP.

## 25 **Introduction**

26 Zooplankton have long been known to undertake vertical migrations, the most commonly  
27 described being diel vertical migration (DVM) (Cushing, 1951). DVM is a phenomenon in  
28 which, classically, zooplankton travel in a synchronised manner to the upper water column  
29 at night to feed, and reside in deeper waters during the day (Lampert, 1989). Although this  
30 behaviour is often thought of simply as a feeding strategy synchronised by external light  
31 (Pearre, 2003), the diversity of migration patterns that have now been resolved suggests  
32 that it may have a number of drivers. For instance, synchronised migration patterns have  
33 been shown to be disrupted or cease altogether in the absence of predators (Gliwicz, 1986)  
34 which supports the view that DVM is a response to predation threat (the predator-  
35 avoidance hypothesis; Stich & Lampert, 1981). Alternatively, individuals may reduce  
36 energetic costs through residing in deeper, colder waters (metabolic advantage hypothesis;  
37 Enright, 1977).

38 In addition to classical DVM, individual zooplankton may make a number of further shorter-  
39 term migrations, or forays, into the surface layers (Pierson et al. 2009). Unlike DVM, these  
40 forays are more likely to be unsynchronised at the population level and hard to detect with  
41 traditional net-sampling and active acoustic methods (Cottier et al., 2006; Pearre, 1979).  
42 These forays could allow individuals to maximise their food intake through numerous short-  
43 term visits to the feeding layers at the surface and sinking to less risky layers during  
44 digestion (hunger-satiation hypothesis; Pearre, 2003). Accordingly, variation between  
45 individuals in feeding and digestion rates, which determines the timings of upwards and  
46 downwards forays, results in a loss of synchronised vertical movement.

47 The vertical movement of zooplankton enhances the export of nutrients and carbon from  
48 the upper to the deeper layers (known as active flux), contributing to the Biological Carbon  
49 Pump (BCP; Turner, 2002). The contribution of this 'active flux' to the total volume of  
50 particulate organic carbon (POC) is poorly parameterised but is thought to vary across  
51 seasons and oceanic regimes (Boyd et al., 2019; Buesseler & Boyd, 2009), with estimates  
52 ranging from 3% (Hernández-León et al., 2001) to 70% (Dam et al., 1995) of the total POC  
53 export and up to 90% of dissolved inorganic carbon export (Boyd et al., 2019). Faecal pellets  
54 produced by zooplankton may contribute significantly to the downward flux of POC (Cavan  
55 et al., 2015; Manno et al., 2015; Turner & Ferrante, 1979). Foray behaviour was found to

56 increase the number of faecal pellets produced below 30 m (a depth at least 10 m below the  
57 highest chlorophyll (Chl-a) values) when compared to a population displaying no migration  
58 patterns (Wallace et al., 2013), suggesting that the presence of this behaviour may act to  
59 increase the contribution of active flux to the BCP. Greater knowledge of the prevalence of  
60 foray behaviour will allow more accurate estimates of the BCP.

61 Although the Southern Ocean (south of 50°S) occupies only 10% of the global ocean area, it  
62 takes up about 20% of the global ocean CO<sub>2</sub> uptake flux and so is a major contributor to the  
63 BCP (Takahashi et al., 2002). Furthermore, high latitude regions undergo the largest changes  
64 in seasonal light regimes with almost continual light during the productive summer period  
65 (Berge et al., 2015). If light is a cue to synchronise zooplankton migration, it is in these  
66 environments that synchronised migration patterns will undergo the greatest seasonal  
67 changes, possibly halting altogether during summer (Blachowiak-Samolyk et al., 2006). This  
68 may initiate greater levels of foray behaviour (Cottier et al., 2006; Wallace et al., 2010), so  
69 continuing the process of active flux.

70 Pierson et al. (2009) attempted to investigate zooplankton foray behaviour using net traps  
71 in Dabob Bay, USA, an inshore bay on the west coast of the USA. Foray behaviour was  
72 observed in *Calanus pacificus* and *Metridia pacificus* females, evidenced by the presence of  
73 individuals in the upward looking nets throughout the night, indicating that a number of  
74 zooplankton were migrating downwards. Furthermore, these individuals had increased gut  
75 contents compared to those caught swimming upwards. Nevertheless, the sampling system  
76 was subject to some methodological biases including a selectivity for downward-migrating  
77 plankton and a bias towards larger individuals in the upward looking net.

78 Although the system of Pierson et al. (2009) was successful in an inshore setting, the more  
79 dynamic environmental conditions of the open ocean, with greater variability in sea state  
80 and wind speeds, provides an even greater challenge. Our study aims to build upon the  
81 work of Pierson et al. (2009) by developing a new net system to detect zooplankton foray  
82 behaviour in the open-ocean environment that will help improve our understanding of  
83 carbon flux in future ecosystem studies. We developed and trialled a novel bi-directional  
84 net, the Motion-compensated Upward and Downward Looking (MUDL) net, with the  
85 intention of quantifying upward and downward travelling zooplankton simultaneously. Our  
86 net system was deployed in the Antarctic Polar Front region of the southwest Atlantic sector

87 of the Southern Ocean, a region where sampling conditions are challenging and very little is  
88 known about foray behaviour in the local zooplankton community. The MUDL net catches  
89 were analysed for taxonomic composition to examine which Southern Ocean zooplankton  
90 species and developmental stages undertake foray behaviour, and to examine possible  
91 regional differences between taxa undertaking this behaviour across different  
92 environmental conditions. Our study aims to demonstrate the utility of the MUDL net for  
93 examining zooplankton behaviour in open ocean environments, which will improve our  
94 understanding of the role of zooplankton vertical migration in vertical carbon flux via the  
95 BCP.

96 **Methods**

97 Net system: The Motion compensated Upward and Downward Looking net (MUDL) was  
98 designed by scientists and engineers at the British Antarctic Survey. The MUDL net is  
99 comprised of two conical nets mounted on an aluminium frame (Figure 1). Both nets have a  
100 rigid cylindrical opening with a diameter of 61 cm, with 100 µm nylon netting tapering to  
101 cod ends 2 m away. The nets are positioned with one net opening looking up and the other  
102 looking down. At the entrance of the cod ends is a spherical valve. This valve is hollow with  
103 three circular holes cut into it and is the mechanism which allows the net to start and end  
104 sampling. The positioning of the valves determines when sampling occurs. In a closed  
105 position, the alignment of the valves results in the cod ends being closed and any water  
106 flushed through the net being released through a side opening in the cod end. Sampling  
107 commences when the valves rotate to an open position by aligning the holes to create an  
108 open passage into the cod ends. After a set time, the valves rotate back into the closed  
109 position ensuring no zooplankton are caught during net retrieval. The valves are rotated via  
110 arms connected to a motor located in the centre of the frame. Prior to deployment, the  
111 motor is programmed to rotate the arms and therefore the valves at set time points. In  
112 addition to the motor, a spring loaded motion compensation mechanism sits in the centre  
113 of the frame. This allows the net to maintain its vertical position and remain stable within  
114 the water column, independent of any ship motion. It is necessary to fill the cod-ends with  
115 water prior to deployment to avoid large differences in environmental conditions within the  
116 cod-ends. This water was taken from Niskin bottles fired at the intended deployment depth  
117 during a prior CTD cast. Further details of the design and sampling protocol are provided in  
118 *Supplementary Information 1*.

119 Sampling protocol: Zooplankton sampling was carried out by deploying the MUDL from the  
120 *RRS James Clark Ross* as part of the British Antarctic Survey (BAS) long-term ecosystem  
121 monitoring programme in the vicinity of South Georgia during austral summer, December  
122 2016-January 2017 (JR16003). The MUDL net was deployed in four locations, to the south  
123 and east of, and within, the Polar Frontal Zone (Figure 2). Stations within the Polar Front  
124 were labelled Polar Front 2 (PF2) and Polar Front 4 (PF4), while the stations to the south of  
125 the Polar Front were labelled P2 and P3.

126 At each station, the MUDL was deployed at two different time points separated by  
127 approximately 12 h. We have nominally categorised these as dusk and dawn although exact  
128 timings vary with regards the relationship to sunrise and sunset (the average time difference  
129 between sunset or sunrise and the start of a deployment was 2 h 20 mins while the  
130 maximum difference was 4 h 16 mins). Dual deployments were made at each time point,  
131 one to a set depth of 100 m and the second to 10 m below the Chl-a maximum (typically 60-  
132 80 m depth) as determined by a prior CTD cast (Table 1). These dual-deployments were  
133 repeated at station P2 where further time was available.

134 A vertical mini-Bongo deployment was made at approximately the same time as the evening  
135 MUDL deployment at station PF4 as a means of comparing the zooplankton community  
136 captured by a traditional net to that by the MUDL (further details on the specification of the  
137 mini-Bongo, its deployment protocol and subsequent sample and statistical analyses are  
138 provided in *Supplementary Information 2*).

139 Environmental sampling: Information on environmental conditions at the time of sampling  
140 was provided by CTD casts. The CTD consisted of a SBE32 carousel water-sampler, a  
141 SBE9Plus CTD, containing a SBE3Plus temperature sensor, a fluorometer (Chelsea  
142 Aquatracker mark III) and a photosynthetically active radiation (PAR) sensor. The depth of  
143 the Chl-a maxima were determined from the Chl-a profile obtained during the downcast  
144 (Figure 3). Water for use in the respective MUDL deployments was obtained from 100 m  
145 and 10 m below the Chl-a maxima during the upcast of the CTD and the cod ends were filled  
146 with this water as close as possible to the time of deployment. The MUDL net was  
147 programmed using customised Hydrobios software, and was set to rotate the valves within  
148 the cod ends to an open position after 12 minutes, allowing it to reach the target depth  
149 before opening. Deployments were made with the valves in a closed position minimising  
150 contamination during this stage. Once the net was at the target depth, the valves rotated to  
151 an open position allowing the mixing of water in the cod ends and zooplankters to swim into  
152 the cod ends. The valves remained in this open position for 20 minutes, before being closed  
153 for retrieval. Whilst open, the MUDL remained at the target depth, and with the aid of the  
154 motion compensating mechanism, vertical movement was minimised, decreasing the  
155 potential of zooplankton to enter the nets through intermittent vertical motions caused by

156 the effect of oceanic swell. The net was hauled vertically to the surface in the closed  
157 position, preventing contamination of the cod-end samples during this phase.

158 Zooplankton sample processing: Once the net had been recovered, the cod ends were  
159 emptied. This was done by opening a tap valve at the base of the upward looking net,  
160 allowing the sample to be collected by placing a large bucket underneath. To collect the  
161 sample from the downward looking net, the base of the net was removed and the valve  
162 rotated to an open position. Once in an open position, the sample was collected in the same  
163 way as the upward looking net. Samples were then passed through a 100 µm nylon mesh  
164 cloth, collecting any zooplankton on the cloth. Mesh cloths were immediately frozen at -80  
165 °C for analysis back at the UK laboratory.

166 Once back at the UK laboratory, frozen samples from the MUDL net deployments were  
167 transferred to ethanol or 4% buffered formaldehyde (within 24 months of collection) and  
168 the samples analysed within days of this fixation. Whole samples were analysed and  
169 zooplankton were counted and taxonomically identified using a stereo microscope  
170 (Olympus SZX16) with a NIKON D750 camera attachment. Photos of zooplankton were taken  
171 to enable secondary verification of taxonomic identification. Easily distinguishable  
172 zooplankton were identified to species, such as *Rhincalanus gigas*, *Calanoides acutus* and  
173 *Calanus propinquus*. Other taxa were identified to genus level, including *Oithona* spp.,  
174 *Metridia* spp. and *Thysanoessa* spp. The remainder were identified to groups including  
175 calanoids, pteropods, ostracods, chaetognaths, euphausiid calyptopes and hyperiid  
176 amphipods.

177 Statistical analyses: To compare species diversity at the various locations, Shannon Diversity  
178 Indices were calculated. Samples were pooled by location for this analysis with all samples  
179 across all depths at each time point pooled to form two locational groups: (1) the Polar  
180 Front group (stations PF2 and PF4) and (2) the P2 group. Due to only having one sample  
181 from P3, this sample was not included in this specific analysis (although details and analyses  
182 of the P3 catch are included where appropriate elsewhere). For each location, this enabled  
183 community structure comparisons between the upward and downward looking nets at both  
184 dusk and dawn. Shannon Diversity Index measures species richness based on the total  
185 number of species found within a population and was calculated as follows:

186

$$187 \quad H' = \sum_{i=1}^R p_i \ln p_i \quad (1)$$

188

189 Where  $p_i$  is the proportion of individuals belonging to each species.

190 Comparisons between abundances within upward looking and downward looking net  
191 catches were made using a non-parametric Mann-Whitney U test, having first failed tests  
192 for either normality or equal variance.

193 A multivariate analysis was conducted using Primer 7 (version 7.0.13, PRIMER-e) (Clarke &  
194 Gorley, 2015). Data were imported in a sample-variable matrix, where each net at each  
195 deployment was a sample and the taxa were variables. In total, 26 samples were included  
196 from 13 net deployments. All samples had corresponding factors of location, time, depth  
197 and net direction.

198 For all analyses, data were fourth root transformed to reduce the influence of highly  
199 abundant taxa. Shade plots were used to confirm such taxa had been sufficiently down-  
200 weighted before proceeding with further analyses (Clarke & Gorley 2015). Subsequently, a  
201 resemblance matrix was generated, calculating Bray-Curtis similarities between samples.

202 The above similarity matrix was analysed through non-metric multidimensional scaling  
203 (nMDS; Kruskal stress formula 1) to provide further context on similarities and differences  
204 between sample sets. nMDS generates ordination plots where the distance between  
205 samples is a representation of the multi-dimensional differences in the underpinning  
206 resemblance matrix.



207 **Results**

208 Environmental context: Temperature, salinity and fluorescence profiles show the differing  
209 environmental conditions at the stations sampled during the cruise (Figure 3). P3 and P2  
210 showed a similar water column structure consisting of a surface mixed layer (~0 to 80 m),  
211 winter water (~80 to 200 m) and then upper circumpolar deep water (UCDW) (below ~200  
212 m). Temperature ranged between -0.5°C and 2°C, reaching a minimum in the winter water  
213 layer and a maximum in the UCDW. Salinity ranged between 33.7 and 34.6, being freshest at  
214 the surface and most saline at depth. At the Polar Front Zone (PF) stations, the structure of  
215 the water column was less clear, most likely as a result of high levels of vertical mixing.  
216 Temperatures were higher than P2 and P3, varying between 2.4 and 3.6°C. Salinity was 33.8  
217 in the upper mixed layer increasing to 34.4 by 500 m. Chl-a derived from fluorescence  
218 measurements reached its maximum value within the surface mixed layer at all locations.  
219 The PF stations and P3 had much greater Chl-a maxima (0.7 and 0.8 mg m<sup>-3</sup> respectively)  
220 than P2 (~ 0.25 mg m<sup>-3</sup>). At P3, the maximum Chl-a was found in the surface 50 m before a  
221 sharp decline to < 0.01 mg m<sup>-3</sup> by 200 m. At P2, a subsurface maximum was present, with  
222 the highest values being around 70 m, followed by a sharp decline to around 0.02 mg m<sup>-3</sup> by  
223 150 m. The same pattern of Chl-a abundance was seen in the PF stations, with subsurface  
224 maxima being present in the mixed layer at ~70 m before declining rapidly to <0.02 mg m<sup>-3</sup>  
225 by 200 m.

226 Performance of MUDL net: All MUDL deployments resulted in zooplankton being caught in  
227 both nets, indicating that the net was effective in catching both upward and downward  
228 swimming zooplankton. However, the upward looking nets caught significantly more than  
229 the downward looking nets (Mann-Whitney U test, P<0.001), with the downward looking  
230 net catching an average of 24% (SD 23%) of the corresponding upward looking net catch  
231 (Figure 4).

232 A mini-Bongo vertical deployment was carried out at PF4 to compare with the PF4 MUDL  
233 deployment. Both devices captured a similar range of organisms, dominated by calanoid and  
234 cyclopoid copepods. However, calanoids were more likely to be captured by the MUDL  
235 compared to their relative prevalence in the water column while cyclopoids were less likely  
236 to be captured (see *Supplementary Information 2* for further details).

237 Analyses of taxa: Across all samples, copepods accounted for over 90% of all organisms in  
238 terms of abundance (Figure 5). Cyclopoids were the most common copepod followed by  
239 calanoids. Cyclopoid dominance was slightly higher in dawn samples than dusk samples,  
240 with taxa such as calanoids, ostracods, annelids and pteropods having a greater  
241 proportional abundance at dusk (Figure 5).

242 The pattern of much higher abundances in the upward looking compared to downward  
243 looking net was apparent both at the PF stations and at station P2 (Fig. 6). However,  
244 between dusk and dawn, abundances in nets of the same direction were comparatively  
245 similar. For instance, across P2 and PF stations, dawn and dusk upward looking nets all had  
246 averages of between 200 and 500 individuals, while averages of downward looking nets  
247 ranged between 40 and 125 individuals. Within these ranges, overall abundance was higher  
248 in the PF stations compared to P2 in both upward and downward looking nets.

249 With regards Shannon diversity, values were greater in the PF stations compared to P2.  
250 Furthermore, the diversity of the community moving at dusk at the PF stations was greater  
251 than at dawn (Dawn: upward looking  $H = 1.72$ , downward looking  $H = 1.84$ , Dusk: upward  
252 looking  $H = 2.13$ , downward looking  $H = 2.24$ ; Figure 6). This was not the case at P2, where  
253 dawn samples had marginally higher Shannon Diversity indices than samples collected at  
254 dusk (Dawn: upward looking  $H = 1.52$ , downward looking  $H = 1.44$ , Dusk: upward looking  $H =$   
255  $1.22$ , downward looking  $H = 1.42$ ).

256 In terms of taxonomic composition, the cyclopoid copepod *Oithona spp.* was found to be  
257 the most dominant genus across all samples (Table 2). The other dominant taxa differed  
258 between P2 and PF stations. At P2, *Oithona*, the calanoid copepod *Ctenocalanus*, pteropods  
259 and nauplii were abundant across both net directions and sampling times while, at the PF  
260 stations, harpacticoid copepods, the calanoids *Metridia* and *Haloptilus*, the cyclopoid  
261 *Oncaea* and pteropods were most abundant. There was little difference in the taxonomic  
262 composition of organisms captured at the depth of the Chl-a max + 10 m compared with  
263 those captured deeper, at 100 m (Table 3). The major difference was the presence of  
264 pteropods in the upward looking net at Chl-a max + 10 m, which were not found at the  
265 deeper depth nor in any downward looking nets.

266 Multivariate analysis of all samples collected during the survey showed two broad groups in  
267 the nMDS plot (Figure 7), separating the downward looking samples from the upward  
268 looking samples. Furthermore, the upward looking samples grouped closer together than  
269 the downward looking samples, indicating a greater degree of variation between  
270 deployments in the latter. In addition, when dawn and dusk samples were analysed without  
271 considering net direction, dawn samples grouped closer together than the dusk samples,  
272 indicating that similarity between dawn samples was comparatively greater. However, there  
273 was a large degree of overlap within the groupings suggesting high variability and the  
274 presence of common taxa across all samples. Location did not have a major influence on the  
275 pattern of grouping despite differences in water column structure between stations.

276 **Discussion**

277 Performance of MUDL net: The system was successful in capturing a range of zooplankton  
278 taxa, swimming both upwards and downwards, at a range of depths within the epipelagic  
279 layers. These taxa were captured swimming in both directions at both dusk and dawn.

280 Our environmental analyses showed particular spatial contrasts in water column structure,  
281 with the Polar Frontal Zone stations (PF2 and PF4) being around 1 to 2°C warmer, and with a  
282 deeper mixed layer compared to the Scotia Sea stations (P2 and P3). Across this range of  
283 conditions, the MUDL successfully captured similar amounts of organisms in both the  
284 upward and downward looking nets, showing that the prevalence of these behaviours was  
285 widespread.

286 Compared to a traditional vertically-deployed mini-Bongo net, the MUDL captured a similar  
287 composition of taxonomic groups, dominated by calanoid and cyclopoid copepods.

288 However, in comparative terms, the more motile calanoids were more likely to be captured  
289 by the MUDL.

290 Net direction bias Within nMDS analyses, the samples formed two groups. Samples from the  
291 upward looking net formed one cluster whilst the other cluster was formed of a majority of  
292 samples from the downward looking net. However, although these groups were broad, with  
293 a high degree of overlap, net direction appeared to be a major driver of multivariate  
294 structure. One explanatory factor may be differences in net capture efficiency between  
295 upward and downward looking nets. The MUDL net consistently caught a larger number of  
296 downward migrating than upward migrating zooplankton, with the downward looking net  
297 catching around a quarter of the corresponding upward looking net catch. It is not clear why  
298 this was the case although this pattern is consistent with Pierson et al., (2009) who also  
299 caught larger numbers in the upward looking net when using net traps similar to those used  
300 in the present study. Pierson et al., (2009) suggested a number of reasons for this, including  
301 differences in behavioural and sensory responses of migrating organisms. For instance,  
302 organisms swimming upwards into the downward looking net may encounter the side  
303 panels of the net as they enter and respond by swimming downwards. If this is the case,  
304 organisms that come into contact with the net at any point during upward migration may  
305 not enter the cod end and hence avoid capture.. Organisms entering the upward looking net

306 may be doing so by passive sinking and may be less inclined to swim upwards and out of the  
307 net on encountering any side panels. In addition to this, if the main response to sensing the  
308 equipment is to swim down, then this will only act to increase the funnelling of naturally  
309 downward swimming organisms into the cod end, resulting in a bias in numbers caught by  
310 the upward looking net.

311 Pierson et al., (2009) further suggested light attenuation caused by the net may be a factor  
312 in reducing the capture efficiency of downward looking nets. As zooplankton migrate  
313 upwards, the net may block or alter the light signal they receive from the surface. This  
314 alteration may result in avoidance behaviour by the zooplankton reducing the capture  
315 efficiency of the downward looking net. If this is the case, a greater difference between the  
316 nets between night and day would be observed. Due to the deployments in this study  
317 occurring at dawn and dusk, it is not possible to resolve this, as light levels may have been  
318 similar at both time points. Irrespective of the different capture efficiency rates, it is clear  
319 from this study that zooplankton are migrating in both directions at these times.

320 Asynchronous migrations The present study found migrations in both directions at both  
321 dawn and dusk, implying that migrations were asynchronous and occurring throughout a  
322 daily cycle, supporting the presence of foray behaviour. Very few studies have successfully  
323 detected foray behaviour due to difficulties in detecting individual zooplankton movements  
324 (Pearre, 2003). However, Pierson et al., (2009, 2013) were able to demonstrate foray  
325 behaviour in the copepods *Calanus pacifica* and *Metridia pacifica*. This was evidenced by  
326 vertical migrations throughout the night, with those individuals migrating downwards  
327 having fuller guts than those migrating upwards, suggesting satiation associated downward  
328 migration, as would be hypothesised by the hunger satiation hypotheses. Gut contents of  
329 individuals caught by the MUDL were not measured in the present study, so direct  
330 attribution to hunger and satiation processes cannot be made. However, the similarity in  
331 migration patterns seen within this study to those carried out by Pierson et al., (2009, 2013)  
332 suggests that similar mechanisms may be responsible.

333 The presence of downward migrating zooplankton at dusk suggests that a number of  
334 zooplankton were in the surface waters during the day. A number of studies have found  
335 vertically migrating zooplankton to be present in the upper water column during daylight  
336 hours (e.g. Irigoien et al., 2004; Ohman et al., 1983; Pearre, 1970, 1973; Sims et al., 2005).

337 Lampert (1989) and Ohman (1990) argue that a flexibility in vertical migration and  
338 potentially a reverse migration is due to the presence of larger invertebrate predators such  
339 as chaetognaths and euphausiids. Predatory chaetognaths and euphausiids were caught in  
340 the MUDL, showing that these taxa were also undergoing vertical migrations and may be  
341 exerting predation pressure upon the zooplankton community.

342 Cyclopoid foray behaviour: The cyclopoid *Oithona spp.* were found to be the most dominant  
343 taxa captured by the MUDL across all locations and were particularly dominant at P2. This  
344 high abundance is in line with previous sampling efforts within the Scotia Sea (Atkinson &  
345 Sinclair, 2000; Ward et al., 2012). The ratio of directional movement of zooplankton at P2  
346 was found to be dependent upon time, and *Oithona spp.*, as the most abundant  
347 zooplankton taxa, often dominated these community level patterns in vertical movements.  
348 Often regarded as the most ubiquitous copepod in many oceans (Bigelow, 1926), *Oithona*  
349 *spp.* are an important component of the zooplankton community and exhibit an omnivorous  
350 diet (Ward & Hirst, 2007). However, little is known about vertical migration behaviour in  
351 *Oithona spp.* Tanimura et al., (2008) investigated the vertical positioning of *Oithona similis*  
352 under sea ice in mid-summer. During 24-hour daylight, *O. similis* undertook a reverse  
353 migration, inhabiting surface waters during the day and migrating to slightly deeper waters  
354 at night (Tanimura et al., 2008). However, a number of authors report no vertical migration  
355 in *Oithona spp.* species over daily (Bogorov, 1946; Irigoien et al., 2004) or seasonal cycles  
356 (Ashjian et al., 2003; Atkinson, 1998). Our study shows that *Oithona spp.* in the Southern  
357 Ocean are undertaking foray style vertical migrations in the water column which would be  
358 difficult to resolve using traditional netting methods.

359 *Oithona spp.* are ambush predators, detecting prey particles from hydrodynamic signals  
360 (Paffenhöfer & Mazzocchi, 2002; Saiz et al., 2003; Svensen & Kiørboe, 2000). However, it has  
361 been reported that signals can only be perceived by stationary *Oithona spp.* (Paffenhöfer &  
362 Mazzocchi, 2002), with individuals passively sinking until prey is detected at which point  
363 they undertake an active 'jump' in order to catch motile and non-motile prey (Kiørboe,  
364 2007). This feeding strategy indicates that vertical movements within the water column are  
365 a necessary part of *Oithona spp.* feeding behaviour and may lead to the observed foray  
366 behaviour. The present study found that, in contrast to previous studies, *Oithona spp.* were  
367 not vertically stable but were moving vertically within the water column at both dawn and

368 dusk, further underlining the presence of foray behaviour. *Oithona similis* have been found  
369 to have a passive sinking speed of  $0.0237 \pm 0.0042 \text{ cm s}^{-1}$  and a mean swimming velocity of  
370  $0.051 \pm 0.030 \text{ cm s}^{-1}$  (Hubareva & Svetlichny, 2016). Using these speeds, it would take *O.*  
371 *similis* between 2 and 3 hours to passively sink the 2 m distance from the top of the upward  
372 looking net to the cod end, but they may be able to swim the distance in 40 minutes. While  
373 this would indicate that *Oithona* could not traverse the 2 m length of the net during the 20  
374 min in which the net was open, those that were already within the net system, i.e. at the  
375 depth where the MUDL came to rest, would be able to travel into the cod ends. In addition  
376 to this, as passive sinking is slower than active swimming, the high numbers of *Oithona spp.*  
377 caught in the present study are likely to have been actively swimming in either an upward or  
378 downward direction, showing that *Oithona spp.* must be undertaking vertical migrations.

379 This study provides strong evidence that *Oithona spp.* are vertically mobile within the water  
380 column at different time points in the day-night cycle. This is an important finding given  
381 their ubiquitous nature and the major position they occupy within global zooplankton  
382 communities and linked processes, including the BCP (Giering 2013).

383 Contribution to carbon flux The present study reveals the existence of widespread foray  
384 behaviour in the zooplankton communities of the Scotia Sea and Polar Frontal Zone. By  
385 migrating from the upper water column to deeper waters, zooplankton transport carbon (as  
386 well as nutrients) deeper in the water column, so contributing to the BCP. Wallace et al.,  
387 (2013) used a model to simulate the volume of carbon exported in faecal pellets from  
388 copepods undergoing different migration patterns, including foray behaviour. These authors  
389 found that, in the absence of any vertical migrations, the resulting carbon export would be  
390 minimal. Foray behaviour increased the volume of faecal pellet production in the deeper  
391 layers although it was less than that generated by DVM. Asynchronous migrations reported  
392 in the present study may therefore enhance the level of carbon flux in this region beyond  
393 that generated by the DVM community. In the Scotia Sea, particulate organic carbon flux is  
394 up to  $22.91 \text{ mg C m}^{-2} \text{ d}^{-1}$  at 2000 m, with much of this being in the form of faecal pellets  
395 (Manno et al., 2015), highlighting the importance of zooplankton migrations in this region.

396 Future outlook As this trapping technique becomes more established, certain improvements  
397 will be required in both the design and implementation of this technique. Longer  
398 deployments would allow a greater representation of slower swimming organisms (e.g.

399 cyclopoids such as *Oithona*) in the catches. Also, deployment at frequent intervals across  
400 the 24 h cycle would allow the influences of classical DVM, reverse DVM, midnight sinking  
401 and daytime avoidance to be accounted for. Technical improvements could be made to alter  
402 the time-intensive way in which cod-ends are filled and emptied. Further technology could  
403 also be integrated onto its robust net frame, particularly autonomous imaging instruments  
404 (Picheral et al 2022). Such devices could provide a simultaneous view of what is in the  
405 community outside of the nets to compare directly with what is captured. To a certain  
406 extent, such imaging devices can also resolve direction of swimming although this is only  
407 over a short distance, as compared to the MUDL which integrates upwards or downwards  
408 movement over the 2 m length of the net.

409 A major advantage of the MUDL is that it captures live organisms displaying a particular  
410 foray behaviour (i.e. upwards or downwards swimming). Quick and sensitive retrieval of  
411 these individuals will allow meaningful physiological measurements to be made, such as on  
412 respiration and gut evacuation rates. This will allow direct comparisons of the respective  
413 states of individuals during the upward and downward phases of forays. For other  
414 individuals within the catch, instant preservation will allow examination of gut contents  
415 before any further substantial amount of digestion has taken place.

416



417 **References**

- 418 Ashjian, C. J., Campbell, R. G., Welch, H. E., Butler, M., & Van Keuren, D. (2003). Annual cycle  
419 in abundance, distribution, and size in relation to hydrography of important copepod  
420 species in the western Arctic Ocean. *Deep-Sea Research Part I: Oceanographic Research*  
421 *Papers*, 50(10–11), 1235–1261. [https://doi.org/10.1016/S0967-0637\(03\)00129-8](https://doi.org/10.1016/S0967-0637(03)00129-8)
- 422 Atkinson, A. (1998). Life cycle strategies of epipelagic copepods in the Southern Ocean.  
423 *Journal of Marine Systems*, 15(1–4), 289–311. [https://doi.org/10.1016/S0924-](https://doi.org/10.1016/S0924-7963(97)00081-X)  
424 [7963\(97\)00081-X](https://doi.org/10.1016/S0924-7963(97)00081-X)
- 425 Atkinson, A., & Sinclair, J. D. (2000). Zonal distribution and seasonal vertical migration of  
426 copepod assemblages in the Scotia Sea. *Polar Biology*, 23(1), 46–58.  
427 <https://doi.org/10.1007/s0030000050007>
- 428 Berge, J., Renaud, P. E., Darnis, G., Cottier, F., Last, K., Gabrielsen, T. M., Johnsen, G., Seuthe,  
429 L., Weslawski, J. M., Leu, E., Moline, M., Nahrgang, J., Søreide, J. E., Varpe, Ø., Lønne, O.  
430 J., Daase, M., & Falk-Petersen, S. (2015). In the dark: A review of ecosystem processes  
431 during the Arctic polar night. *Progress in Oceanography*, 139, 258–271.  
432 <https://doi.org/10.1016/j.pocean.2015.08.005>
- 433 Bigelow, H. B. (1926). Plankton of the offshore waters of the Gulf of Maine. In *Plankton of*  
434 *the offshore waters of the Gulf of Maine*. (Vol. 968).  
435 <https://doi.org/10.5962/bhl.title.4192>
- 436 Blachowiak-Samolyk, K., Kwasniewski, S., Richardson, K., Dmoch, K., Hansen, E., Hop, H.,  
437 Falk-Petersen, S., & Mouritsen, L. T. (2006). Arctic zooplankton do not perform diel  
438 vertical migration (DVM) during periods of midnight sun. *Marine Ecology Progress*  
439 *Series*, 308, 101–116. <https://doi.org/10.3354/meps308101>
- 440 Bogorov, B. G. (1946). Peculiarities of diurnal vertical migrations of zooplankton in polar  
441 seas. *Journal of Marine Research*, 6(1), 25–33.
- 442 Boyd, P. W., Claustre, H., Levy, M., Siegel, D. A., & Weber, T. (2019). Multi-faceted particle  
443 pumps drive carbon sequestration in the ocean. *Nature*, 568(7752), 327–335.  
444 <https://doi.org/10.1038/s41586-019-1098-2>

445 Buesseler, K. O., & Boyd, P. W. (2009). Shedding light on processes that control particle  
446 export and flux attenuation in the twilight zone of the open ocean. *Limnology and*  
447 *Oceanography*, 54(4), 1210–1232. <https://doi.org/10.4319/lo.2009.54.4.1210>

448 Cavan, E. L., Le Moigne, F. A. C., Poulton, A. J., Tarling, G. A., Ward, P., Daniels, C. J., Fragoso,  
449 G. M., & Sanders, R. J. (2015). Attenuation of particulate organic carbon flux in the  
450 Scotia Sea, Southern Ocean, is controlled by zooplankton fecal pellets. *Geophysical*  
451 *Research Letters*, 42(3), 821–830. <https://doi.org/10.1002/2014GL062744>

452 Clarke, K. R., & Gorley, R. N. (2015). Getting started with PRIMER v7: user manual/tutorial.  
453 *PRIMER-E: Plymouth, Plymouth Marine Laboratory*, 20 (1).

454 Cottier, F. R., Tarling, G. A., Wold, A., & Falk-Petersen, S. (2006). Unsynchronized and  
455 synchronized vertical migration of zooplankton in a high arctic fjord. *Limnology and*  
456 *Oceanography*, 51(6), 2586–2599. <https://doi.org/10.4319/lo.2006.51.6.2586>

457 Cushing, D. H. (1951). the Vertical Migration of Planktonic Crustacea. *Biological Reviews*,  
458 26(2), 158–192. <https://doi.org/10.1111/j.1469-185X.1951.tb00645.x>

459 Dam, H. G., Zhang, X., Butler, M., & Roman, M. R. (1995). Mesozooplankton grazing and  
460 metabolism at the equator in the central Pacific: Implications for carbon and nitrogen  
461 fluxes. *Deep-Sea Research Part II*, 42(2–3), 735–756. [https://doi.org/10.1016/0967-](https://doi.org/10.1016/0967-0645(95)00036-P)  
462 [0645\(95\)00036-P](https://doi.org/10.1016/0967-0645(95)00036-P)

463 Enright, J. T. (1977). Diurnal vertical migration: Adaptive significance and timing. Part 1.  
464 Selective advantage: A metabolic model. *Limnology and Oceanography*, 22(5), 856–  
465 872. <https://doi.org/10.4319/lo.1977.22.5.0856>

466 Giering, S. L. C. (2013) The role of mesozooplankton in the biological carbon pump of the  
467 North Atlantic. *PhD Thesis. University of Southampton*, pp. 149.

468 Gliwicz, M. Z. (1986). Predation and the evolution of vertical migration behavior in  
469 zooplankton. *Nature*, 320(6064), 746–748.

470 Hernández-León, S., Gómez, M., Pagazaurtundua, M., Portillo-Hahnefeld, A., Montero, I., &  
471 Almeida, C. (2001). Vertical distribution of zooplankton in Canary Island waters:  
472 Implications for export flux. *Deep-Sea Research Part I: Oceanographic Research Papers*,

473 48(4), 1071–1092. [https://doi.org/10.1016/S0967-0637\(00\)00074-1](https://doi.org/10.1016/S0967-0637(00)00074-1)

474 Hubareva, E. S., & Svetlichny, L. S. (2016). Copepods *Oithona similis* and *Oithona davisae*:  
475 Two Strategies of Ecological-Physiological Adaptation in the Black Sea. *Oceanology*,  
476 56(2), 258–265. <https://doi.org/10.1134/S0001437016020089>

477 Irigoien, X., Hulsman, J., & Harris, R. P. (2004). Global biodiversity patterns of marine  
478 phytoplankton and zooplankton. *Nature*, 429(6994), 863–867.  
479 <https://doi.org/10.1038/nature02593>

480 Kiørboe, T. (2007). Mate finding, mating, and population dynamics in a planktonic copepod  
481 *Oithona davisae*: There are too few males. *Limnology and Oceanography*, 52(4), 1511–  
482 1522. <https://doi.org/10.4319/lo.2007.52.4.1511>

483 Lampert, W. (1989). The Adaptive Significance of Diel Vertical Migration of Zooplankton. In  
484 *Functional Ecology* (Vol. 3). <https://doi.org/10.2307/2389671>

485 Manno, C., Stowasser, G., Enderlein, P., Fielding, S., & Tarling, G. A. (2015). The contribution  
486 of zooplankton faecal pellets to deep-carbon transport in the Scotia Sea (Southern  
487 Ocean). *Biogeosciences*, 12(6), 1955–1965. <https://doi.org/10.5194/bg-12-1955-2015>

488 Ohman, M. D. (1990). The Demographic Benefits of Diel Vertical Migration by Zooplankton.  
489 *Ecological Monographs*, 60(3), 257–281. <https://doi.org/10.2307/1943058>

490 Ohman, M. D., Frost, B. W., & Cohen, E. B. (1983). Reverse diel vertical migration: An escape  
491 from invertebrate predators. *Science*, 220(4604), 1404–1407.  
492 <https://doi.org/10.1126/science.220.4604.1404>

493 Orsi, A. H., Whitworth III, T., & Nowlin Jr, W. D. (1995). On the meridional extent and fronts  
494 of the Antarctic Circumpolar Current. *Deep Sea Research Part I: Oceanographic*  
495 *Research Papers*, 42(5), 641–673. [https://doi.org/10.1016/0967-0637\(95\)00021-W](https://doi.org/10.1016/0967-0637(95)00021-W)

496 Paffenhöfer, G. A., & Mazzocchi, M. G. (2002). On some aspects of the behaviour of *Oithona*  
497 *plumifera* (Copepoda: Cyclopoida). *Journal of Plankton Research*, 24(2), 129–135.  
498 <https://doi.org/10.1093/plankt/24.2.129>

499 Pearre, S. (1970). *Light responses and feeding behavior of Sagitta elegans Verrill*.

500 Pearre, S. (1973). Vertical Migration and Feeding in *Sagitta Elegans Verrill*. *Ecology*, 54(2),

501 300–314. <https://doi.org/10.2307/1934338>

502 Pearre, S. (1979). Problems of detection and interpretation of vertical migration. *Journal of*  
503 *Plankton Research*, 1(1), 29–44. <https://doi.org/10.1093/plankt/1.1.29>

504 Pearre, S. (2003, February). Eat and run? The hunger/satiation hypothesis in vertical  
505 migration: History, evidence and consequences. *Biological Reviews of the Cambridge*  
506 *Philosophical Society*, Vol. 78, pp. 1–79. <https://doi.org/10.1017/S146479310200595X>

507 Picheral, M., Catalano, C., Brousseau, D., Claustre, H., Coppola, L., Leymarie, E., Coindat, J.,  
508 Dias, F., Fevre, S., Guidi, L. and Irisson, J.O., Legendre, L., Lombard, F., Mortier, L.,  
509 Penkerch, C., Rogge, A., Schmechtig, C., Thibault, S., Tixier, T., Waite, A., & Stemmann,  
510 L. (2022). The Underwater Vision Profiler 6: an imaging sensor of particle size spectra  
511 and plankton, for autonomous and cabled platforms. *Limnology and Oceanography:*  
512 *Methods*, 20(2), 115-129. <https://doi.org/10.1002/lom3.10475>

513 Pierson, J. J., Frost, B. W., & Leising, A. W. (2013). Foray foraging behavior: Seasonally  
514 variable, food-driven migratory behavior in two calanoid copepod species. *Marine*  
515 *Ecology Progress Series*, 475, 49–64. <https://doi.org/10.3354/meps10116>

516 Pierson, J. J., Frost, B. W., Thoreson, D., Leising, A. W., Postel, J. R., & Nuwer, M. (2009).  
517 Trapping migrating zooplankton. *Limnology and Oceanography: Methods*, 7, 334–346.  
518 <https://doi.org/10.4319/lom.2009.7.334>

519 Saiz, E., Calbet, A., & Broglio, E. (2003). Effects of small-scale turbulence on copepods: The  
520 case of *Oithona davisae*. *Limnology and Oceanography*, 48(3), 1304–1311.  
521 <https://doi.org/10.4319/lo.2003.48.3.1304>

522 Sims, D. W., Southall, E. J., Tarling, G. A., & Metcalfe, J. D. (2005). Habitat-specific normal  
523 and reverse diel vertical migration in the plankton-feeding basking shark. *Journal of*  
524 *Animal Ecology*, 74(4), 755–761. <https://doi.org/10.1111/j.1365-2656.2005.00971.x>

525 Stich, H. B., & Lampert, W. (1981). Predator evasion as an explanation of diurnal vertical  
526 migration by zooplankton. *Nature*, 293(5831), 396–398.  
527 <https://doi.org/10.1038/293396a0>

528 Svensen, C., & Kiørboe, T. (2000). Remote prey detection in *Oithona similis*:

529 Hydromechanical versus chemical cues. *Journal of Plankton Research*, 22(6), 1155–  
530 1166. <https://doi.org/10.1093/plankt/22.6.1155>

531 Takahashi, T., Sutherland, S. C., Sweeney, C., Poisson, A., Metz, N., Tilbrook, B., Bates, N.,  
532 Wanninkhof, R., Feely, R. A., Sabine, C., Olafsson, J., & Nojiri, Y. (2002). Global sea-air  
533 CO<sub>2</sub> flux based on climatological surface ocean pCO<sub>2</sub>, and seasonal biological and  
534 temperature effects. *Deep-Sea Research Part II: Topical Studies in Oceanography*, 49(9–  
535 10), 1601–1622. [https://doi.org/10.1016/S0967-0645\(02\)00003-6](https://doi.org/10.1016/S0967-0645(02)00003-6)

536 Tanimura, A., Hattori, H., Miyamoto, Y., Hoshiai, T., & Fukuchi, M. (2008). Diel changes in  
537 vertical distribution of *Oithona similis* (Cyclopoida) and *Oncaea curvata*  
538 (Poecilostomatoida) under sea ice in mid-summer near Syowa Station, Antarctica. *Polar*  
539 *Biology*, 31(5), 561–567. <https://doi.org/10.1007/s00300-007-0388-6>

540 Trathan, P. N., Brandon, M. A., Murphy, E. J., & Thorpe, S. E. (2000). Transport and structure  
541 within the Antarctic Circumpolar Current to the north of South Georgia. *Geophysical*  
542 *Research Letters*, 27(12), 1727–1730. <https://doi.org/10.1029/1999GL011131>

543 Turner, J. T. (2002). Zooplankton fecal pellets, marine snow and sinking phytoplankton  
544 blooms. *Aquatic Microbial Ecology*, 27(1), 57–102. <https://doi.org/10.3354/ame027057>

545 Turner, J. T., & Ferrante, J. G. (1979). Zooplankton Fecal Pellets in Aquatic Ecosystems.  
546 *BioScience*, 29(11), 670–677. <https://doi.org/10.2307/1307591>

547 Wallace, M. I., Cottier, F. R., Berge, J., Tarling, G. A., Griffiths, C., & Brierley, A. S. (2010).  
548 Comparison of zooplankton vertical migration in an ice-free and a seasonally ice-  
549 covered Arctic fjord: An insight into the influence of sea ice cover on zooplankton  
550 behavior. *Limnology and Oceanography*, 55(2), 831–845.  
551 <https://doi.org/10.4319/lo.2010.55.2.0831>

552 Wallace, M. I., Cottier, F. R., Brierley, A. S., & Tarling, G. A. (2013). Modelling the influence of  
553 copepod behaviour on faecal pellet export at high latitudes. *Polar Biology*, 36(4), 579–  
554 592. <https://doi.org/10.1007/s00300-013-1287-7>

555 Ward, P., Atkinson, A., & Tarling, G. (2012). Mesozooplankton community structure and  
556 variability in the Scotia Sea: A seasonal comparison. *Deep-Sea Research Part II: Topical*  
557 *Studies in Oceanography*, 59–60, 78–92. <https://doi.org/10.1016/j.dsr2.2011.07.004>

558 Ward, P., & Hirst, A. G. (2007). *Oithona similis* in a high latitude ecosystem: Abundance,  
559 distribution and temperature limitation of fecundity rates in a sac spawning copepod.  
560 *Marine Biology*, 151(3), 1099–1110. <https://doi.org/10.1007/s00227-006-0548-1>

561

562 **Acknowledgements**

563 We are grateful to the officers and crew of the *RRS James Clark Ross* for ably assisting with  
564 deployment of the MUDL net during cruise JR6003. Engineers Scott Palfrey, Dan Ashurst and  
565 Peter Enderlein helped design and construct the net and assisted with deployments. Peter  
566 Ward provided invaluable taxonomic training to VDF and further quality control on the  
567 identification of zooplankton captured by the MUDL. The contribution of GAT and RAS was  
568 supported by the NERC National Capability for sustained observations POETS programme  
569 carried out by the Ecosystems team at the British Antarctic Survey. VDF was funded by the  
570 EnvEast Doctoral Training Partnership.

571

572

573 **Figure legends**

574 Figure 1: MUDL net being deployed from the *RRS James Clark Ross* in the Southern Ocean.  
575 The main features of the net are indicated, including the motion compensatory system and  
576 bi-directional nets.

577 Figure 2: Map of Polar Front region close to South Georgia, showing the four stations where  
578 MUDL deployments were carried out from *RRS James Clark Ross* during 2016/17. Hatched  
579 area shows location of the Polar Front Zone as determined by Orsi et al. (1995) and Trathan  
580 et al. (2000). SACCF – Southern Antarctic Circumpolar Current Front

581 Figure 3: Example profiles of temperature (red line), salinity (blue line) and fluorescence  
582 (green line) with depth as recorded by CTD casts at P3, P2, PF2 and PF4. Horizontal lines  
583 indicate depth of MUDL deployment (Chl-a max + 10 m and/or 100 m). Note different  
584 depths of Chl-a max + 10 m at station P2 resulted from being matched to different CTD  
585 casts.

586 Figure 4: Abundance of organisms identified in upward looking and downward looking nets  
587 across all MUDL deployments carried out during 2016/17. The boundaries of the box  
588 indicate the 25<sup>th</sup> and 75<sup>th</sup> percentiles, the line within box, the median, the whiskers, the  
589 90<sup>th</sup> and 10<sup>th</sup> percentiles, and the dots, 5<sup>th</sup> and 95<sup>th</sup> percentiles.

590 Figure 5: Percentage of individuals captured per taxa across all MUDL deployments. Each  
591 stacked bar represent all deployments grouped together based on deployment time  
592 irrespective of location or depth.

593 Figure 6: Abundance of individuals captured per taxa across all MUDL deployments at P2  
594 (left) and combined PF stations (right). Each stacked bar represent all deployments grouped  
595 together based on deployment time irrespective of depth. Numbers on top of stacked bars  
596 represent Shannon's Diversity Index for each grouping (note that the Diversity Index is  
597 based on lowest taxonomic level within the dataset of which some categories are grouped  
598 here for presentation purposes).

599 Figure 7: nMDS (non-metric Multidimensional Scaling) of all MUDL samples. Spacing  
600 between samples indicates the level of similarity, with those being located closest together  
601 having the greatest similarity. Blue symbols denote samples caught by the upward looking



602 net; green symbols, by the downward looking net. Solid symbols represent dusk samples,  
603 unfilled symbols, dawn samples.

604

605 **Tables**

606 Table 1: MUDL deployments during cruise JR16003, December 2016 to January 2017 (in  
 607 Local Time, GMT-3). Local sunset and sunrise based on times generated by the NOAA Solar  
 608 Calculator <https://gml.noaa.gov/grad/solcalc/sunrise.html>

Depth (m)		Station	Deployment commencement	Deployment Finish Local	Local sunset	Local sunrise
100	Preset Depth	P3	21:13 29/12/16	21:44 29/12/16	03:55	20:46
80	Chl-a max + 10 m	P2	23:24 30/12/16	00:02 31/12/16	03:37	20:58
100	Preset Depth	P2	00:13 31/12/16	00:54 31/12/16	03:37	20:58
80	Chl-a max + 10 m	P2	05:09 31/12/16	05:50 31/12/16	03:37	20:58
100	Preset Depth	P2	05:56 31/12/16	06:38 31/12/16	03:38	20:58
100	Preset Depth	P2	07:05 1/1/17	07:44 1/1/17	03:39	20:57
60	Chl-a max + 10 m	P2	07:55 1/1/17	08:32 1/1/17	03:39	20:57
100	Preset Depth	PF2	22:05 2/1/17	22:43 2/1/17	03:28	20:37
80	Chl-a max + 10 m	PF2	22:52 2/1/17	23:29 2/1/17	03:28	20:37
100	Preset Depth	PF2	06:19 3/1/17	06:59 3/1/17	03:31	20:36
80	Chl-a max + 10 m	PF2	07:08 3/1/17	07:49 3/1/17	03:31	20:36
100	Preset Depth	PF4	21:43 4/1/17	22:20 4/1/17	03:20	20:16
100	Preset Depth	PF4	04:41 5/1/17	05:24 5/1/17	03:21	20:15

609

610

611 Table 2: Most numerous taxa, in order of abundance, within upward looking and downward  
 612 looking nets for a) P2 and b) PF stations. Numbers in brackets denote the average  
 613 abundance ( $\pm$  SD) across all deployments at dusk and dawn in units of individuals per net

614 a)

P2	Dawn	Dusk
Downward looking net	<i>Oithona</i> spp. (40.8 $\pm$ 14.6) Unknown (copepod) (2.8 $\pm$ 3.0) <i>Ctenocalanus</i> spp. (8.3 $\pm$ 4.5) Pteropod (4 $\pm$ 1.2) Nauplii (2 $\pm$ 1.3)	<i>Oithona</i> spp. (13.5 $\pm$ 28.2) Unknown (copepod) (5.5 $\pm$ 2.1) Nauplii (0 $\pm$ 0.7) <i>C. acutus</i> (0.5 $\pm$ 0.7) <i>R. gigas</i> (1 $\pm$ 0.7)
Upward looking net	<i>Oithona</i> spp. (314 $\pm$ 82.4) Unknown (copepod) (16 $\pm$ 22.5) <i>Ctenocalanus</i> spp. (51 $\pm$ 10.3) Pteropod (51.5 $\pm$ 6.4) <i>Oncaea</i> spp. (21.3 $\pm$ 6.1) <i>Metridia</i> spp. (39.8 $\pm$ 5.5)	<i>Oithona</i> spp. (177 $\pm$ 93.36) Unknown (copepod) (39.5 $\pm$ 1.4) <i>Ctenocalanus</i> spp. (34.5 $\pm$ 9.2) Nauplii (4.5 $\pm$ 6.4) Pteropod (7.5 $\pm$ 3.5)

615

616 b)

PF	Dawn	Dusk
Downward looking net	<i>Oithona</i> spp. (37.7 $\pm$ 32.7) Harpacticoid (8.0 $\pm$ 13.9) <i>Ctenocalanus</i> spp. (6.0 $\pm$ 4.6) <i>Metridia</i> spp. (5.0 $\pm$ 5.0) <i>Halyoptus</i> spp. (3.3 $\pm$ 5.8)	<i>Oithona</i> spp. (17.7 $\pm$ 25.4) <i>Oncaea</i> spp. (8.7 $\pm$ 12.5) <i>Metridia</i> spp. (7.0 $\pm$ 5.61) <i>Ctenocalanus</i> spp. (5.3 $\pm$ 6.8) Calanoid (unidentified) (7.5 $\pm$ 7.8)
Upward looking net	<i>Oithona</i> spp. (291.67 $\pm$ 177.46) <i>Ctenocalanus</i> spp. (43.33 $\pm$ 4.9) Pteropod (28.3 $\pm$ 23.5) <i>Metridia</i> spp. (17.7 $\pm$ 21.953) Unknown (copepod) (15.3 $\pm$ 11.3)	<i>Oithona</i> spp. (203 $\pm$ 1629) <i>Ctenocalanus</i> spp. (54 $\pm$ 23.9) Pteropod (45.3 $\pm$ 66.5) <i>Metridia</i> spp. (41.3 $\pm$ 43.2) <i>Oncaea</i> spp. (33.0 $\pm$ 18.19)

617

618

619

620

621 Table 3: Most numerous taxa, in order of abundance, across all MUDL samples collected at  
 622 Chl-a max + 10 m and at 100 m. Numbers in brackets denote the average abundance ( $\pm$  SD)  
 623 across all deployments at that depth in units of individuals per net.

624

	Chl-a max + 10m	100 m
Downward looking net	<i>Oithona spp.</i> (35.6 $\pm$ 22.5) <i>Ctenocalanus spp.</i> (6.8 $\pm$ 5.9) <i>Oncaea spp.</i> (5.2 $\pm$ 10.0) Unknown (copepod) (4.8 $\pm$ 3.6) <i>Metridia spp.</i> (3.8 $\pm$ 5.0)	<i>Oithona spp.</i> (25.8 $\pm$ 22.4) Unknown (copepod) (5.6 $\pm$ 3.4) Harpacticoid (3.1 $\pm$ 8.4) <i>Metridia spp.</i> (2.7 $\pm$ 4) <i>Oncaea spp.</i> (1.2 $\pm$ 1.6)
Upward looking net	<i>Oithona spp.</i> (243.3 $\pm$ 130.9) Pteropod (38.8 $\pm$ 50.5) <i>Ctenocalanus spp.</i> (36.8 $\pm$ 25.8) Unknown (copepod) (31.0 $\pm$ 15.1) <i>Metridia spp.</i> (22.4 $\pm$ 38.6)	<i>Oithona spp.</i> (176.4 $\pm$ 126.1) <i>Ctenocalanus spp.</i> (25.2 $\pm$ 20.4) Unknown (copepod) (18.3 $\pm$ 13.0) <i>Oncaea spp.</i> (12.0 $\pm$ 11.7) <i>Metridia spp.</i> (10.4 $\pm$ 15.2)

625

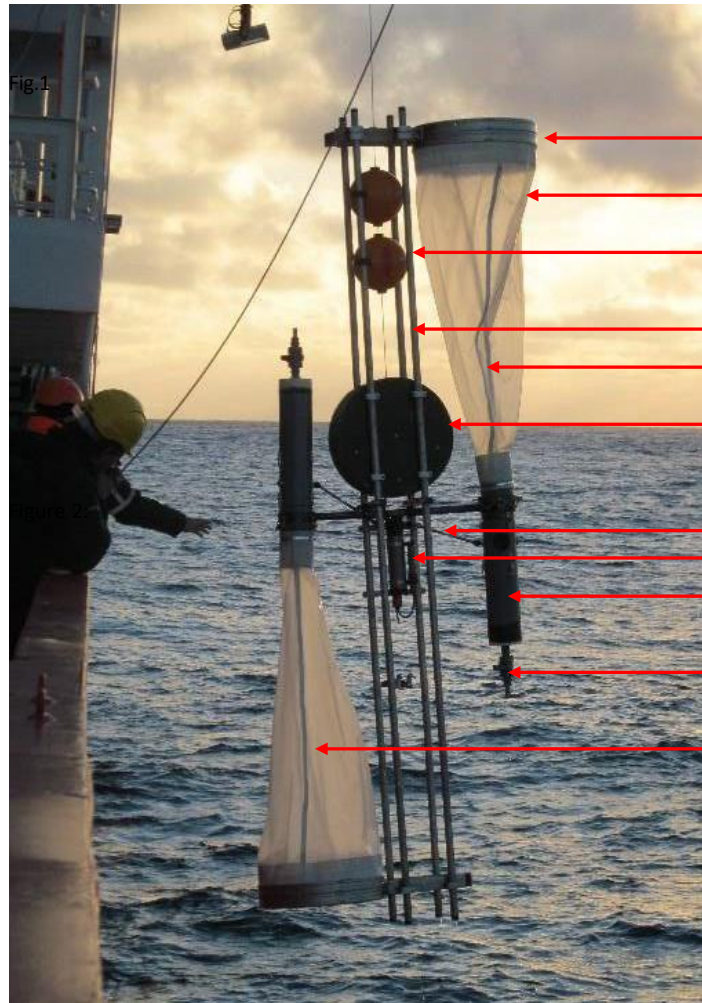


Fig. 1

- ← Net opening
- ← 100  $\mu\text{m}$  mesh
- ← Buoyancy floats (attached to frame)
- ← MUDL Frame
- ← **Upward looking net**
- ← Spring loaded motion compensatory system containing deployment wire
- ← Motor arm
- ← Motor
- ← Cod end
- ← Tap
- ← **Downward looking net**

Fig. 1

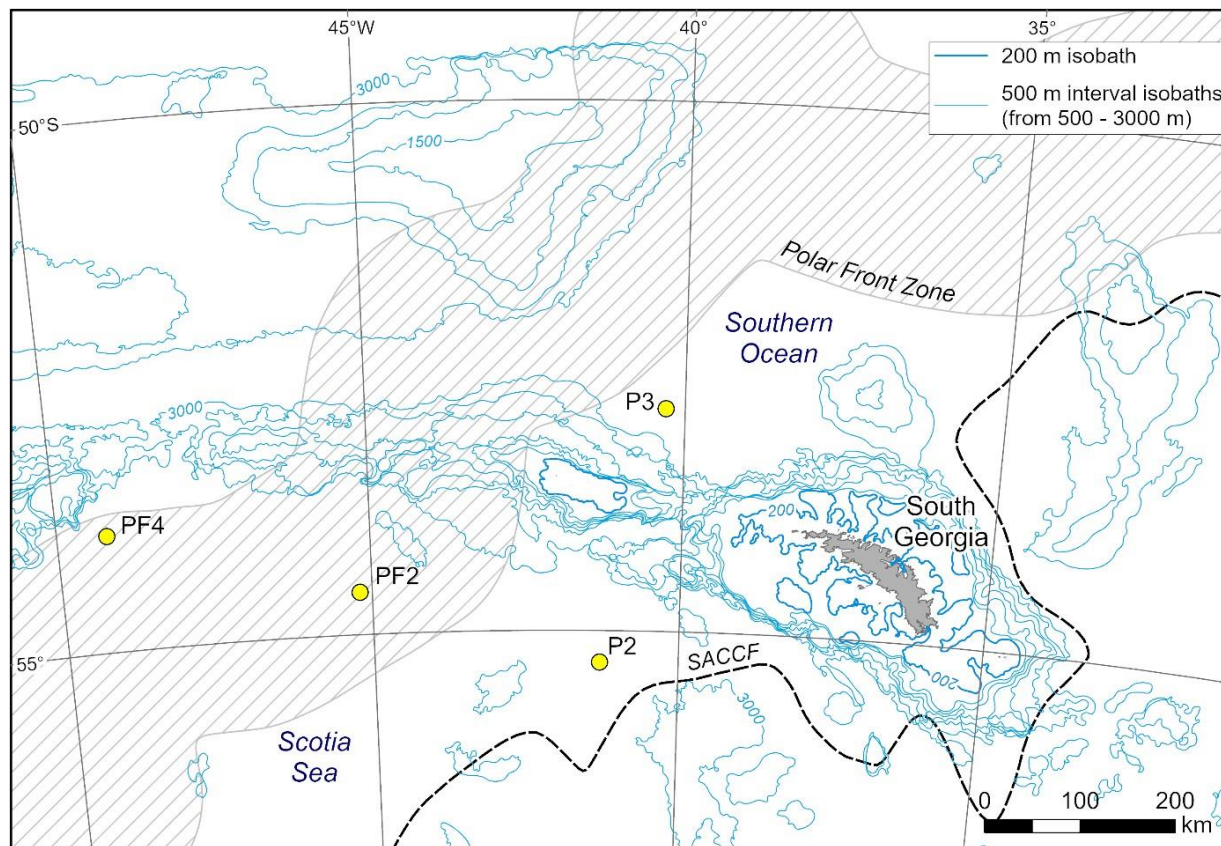


Fig. 2

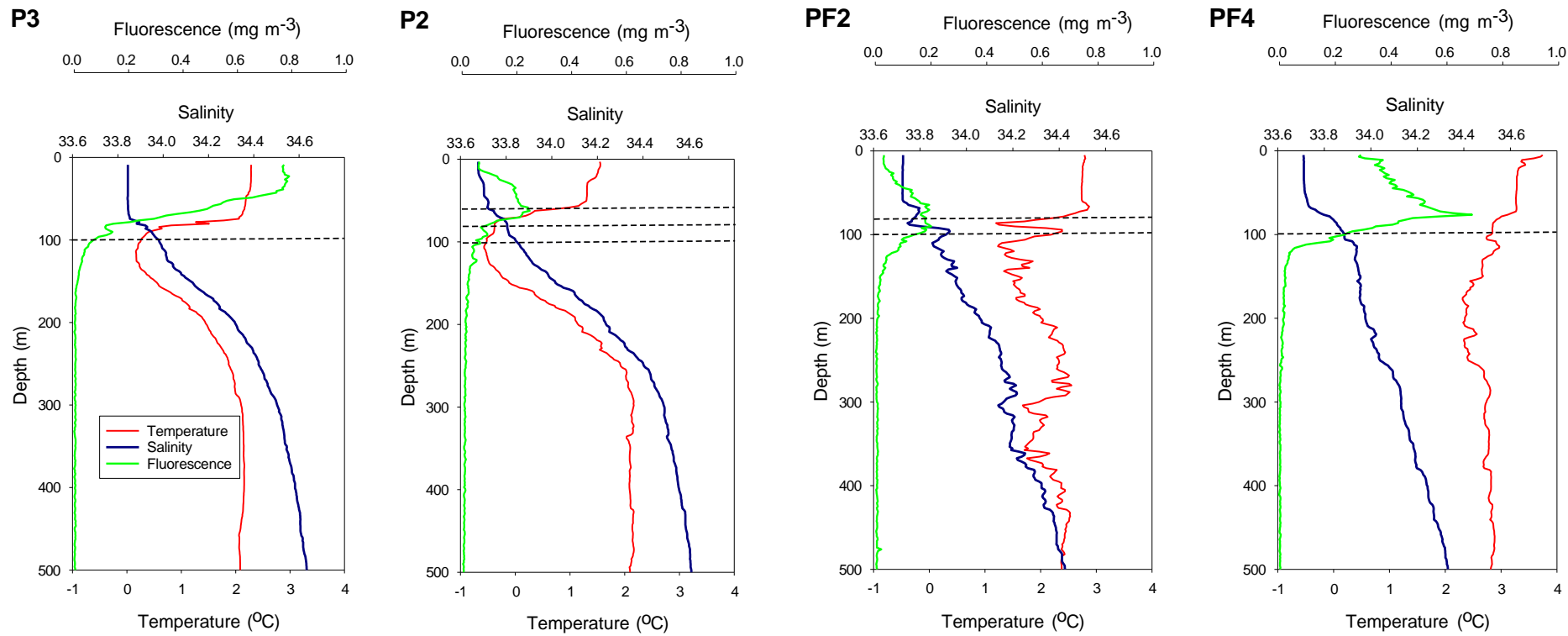


Fig. 3

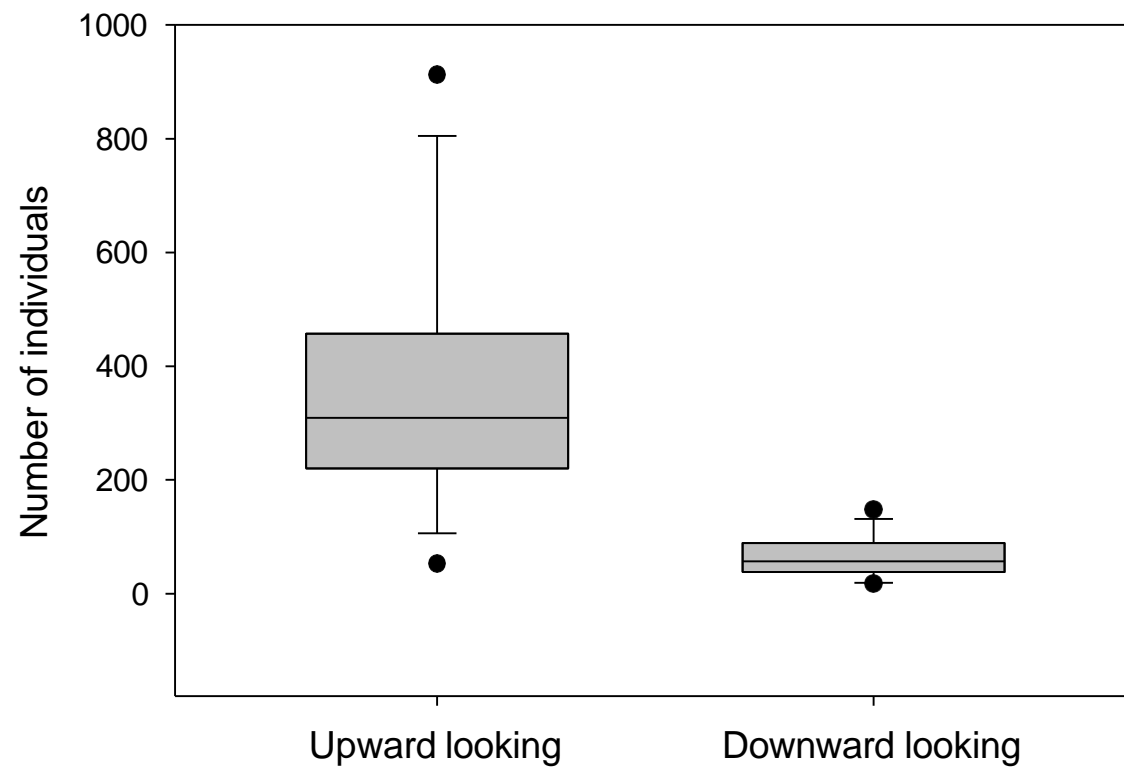


Fig. 4



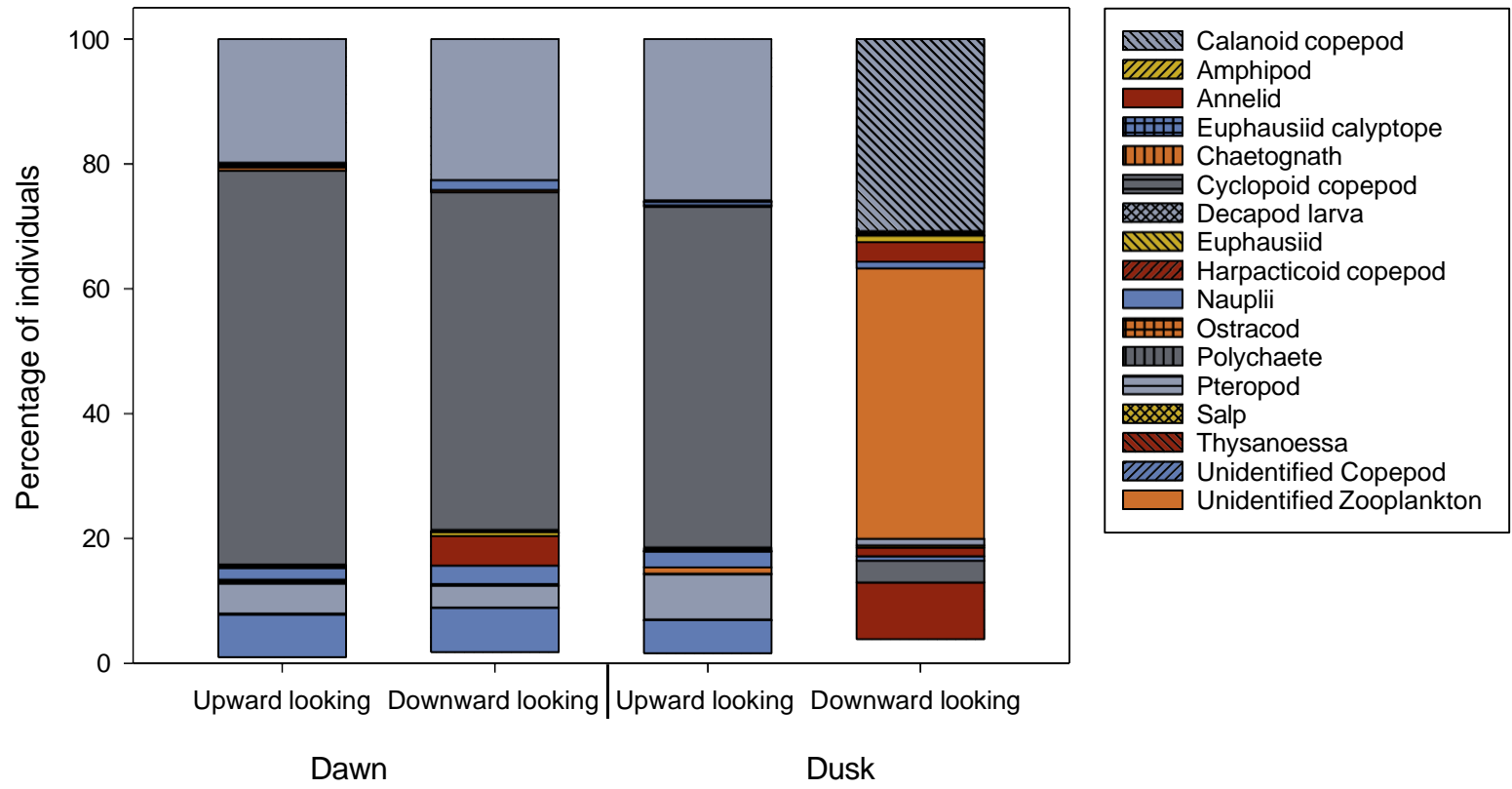


Fig. 5

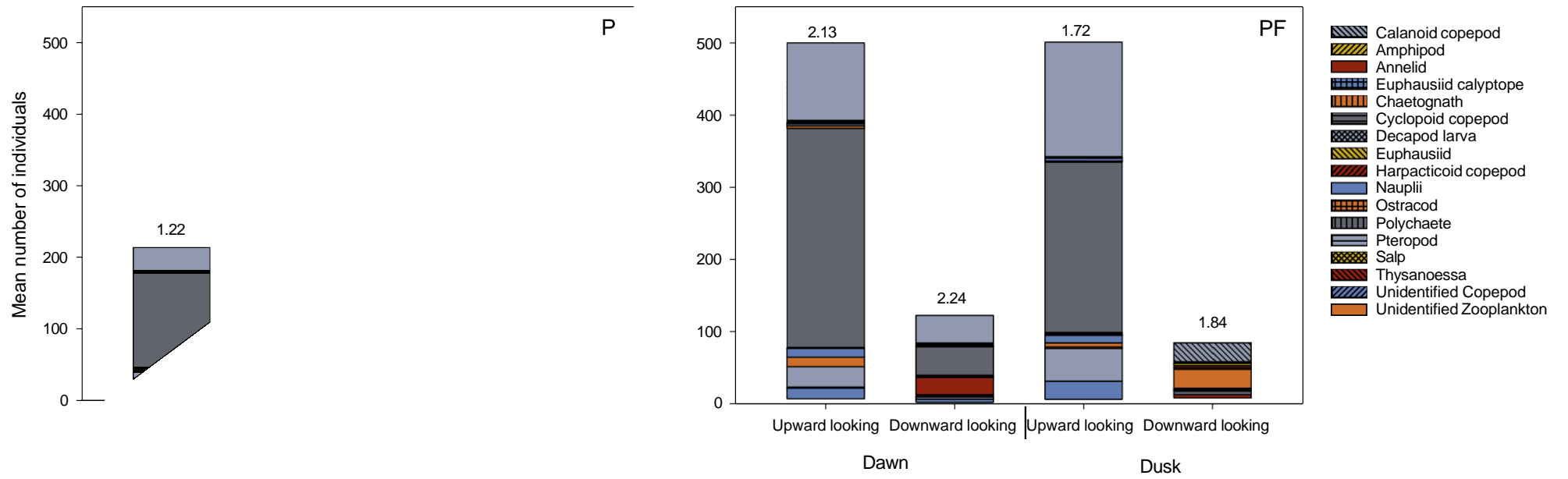


Fig. 6

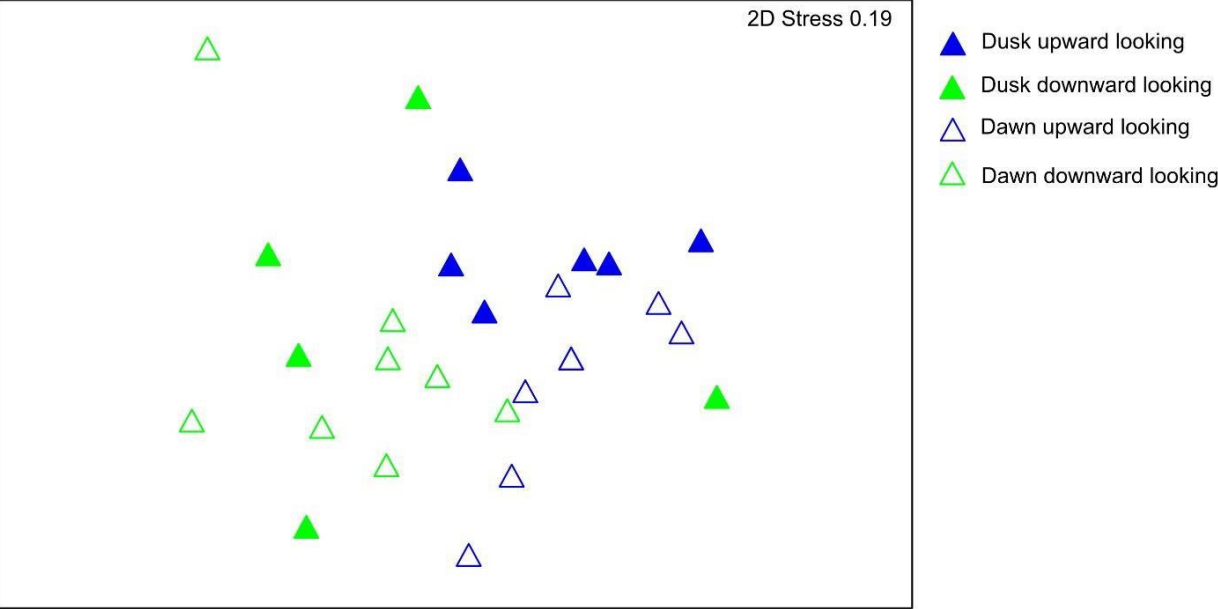


Fig. 7

## Supplementary Information 1: Further technical details of the Motion compensated Upward and Downward Looking (MUDL) net

Victoria Dewar-Fowler<sup>1</sup>, Carol Robinson<sup>2</sup>, Ryan A. Saunders<sup>1</sup>, Geraint A. Tarling<sup>1\*</sup>

1. British Antarctic Survey, High Cross, Madingley Rd, Cambridge, CB3 0ET, UK

2. School of Environmental Sciences, University of East Anglia, Norwich, NR4 7TJ, UK

\* corresponding author

The Motion compensated Upward and Downward Looking (MUDL) net was designed by scientists and engineers at the British Antarctic Survey. It is comprised of two conical nets mounted on an aluminium frame with the deployment wire attached to a spring loaded mechanism (Figure SI1.1). It is deployed tethered to a deployment wire that lowers it to a predetermined depth where it remains for a set period before recovery back onto deck. The purpose of the MUDL is to trap mesozooplankton that enter the net through their own upwards or downwards swimming. This type of trapping allows the level of simultaneous upward and downward flux of these organisms to be determined over a designated period of time.

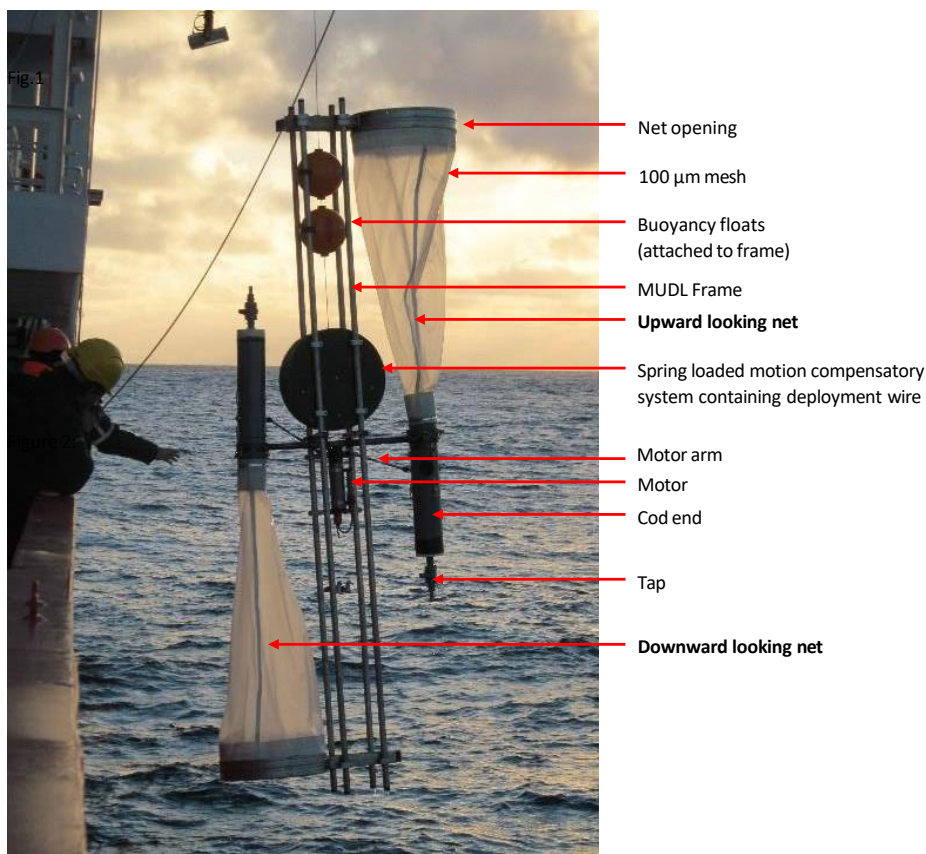
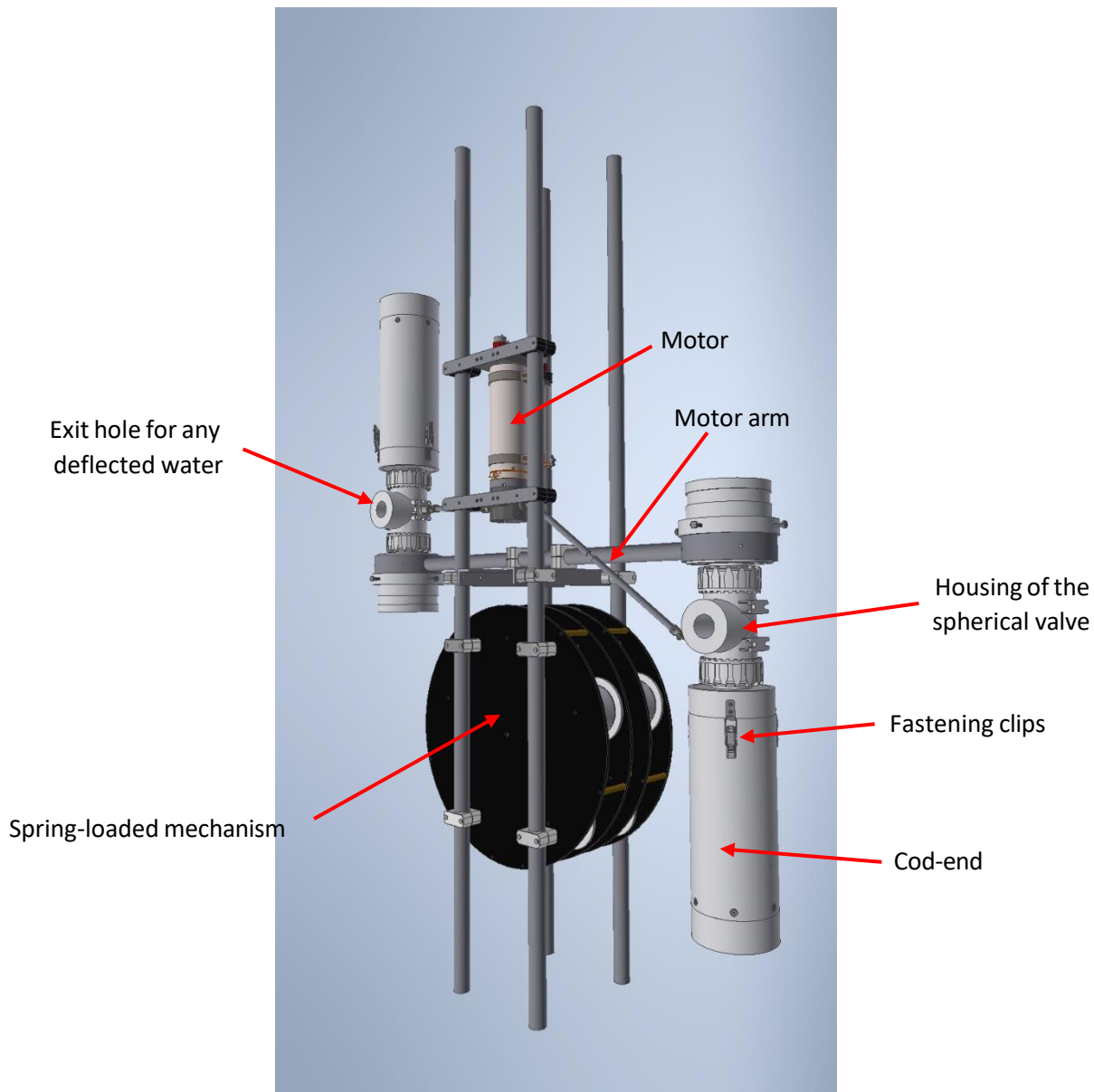


Fig. SI1.1. Motion compensated Upward and Downward Looking (MUDL) net being deployed in Scotia Sea (Dec 2016)

Both the upward-looking and downward-looking nets have a rigid cylindrical opening with a diameter of 61 cm, with a 100  $\mu$ m nylon netting tapering to cod ends 2 m away. The spring loaded motion compensation mechanism that sits in the centre of the frame allows the net to maintain its vertical position and remain stable during deployment. In essence, it compensates for the effect of swell on the deployment vessel that would otherwise be transmitted down the deployment wire to which the MUDL remains tethered throughout the period of deployment. Buoyancy floats positioned towards the upper part of the main frame are there to keep the MUDL as vertical as possible during deployment.



*Fig. S11.2: Schematic of the cod-end mechanism (NB. Taps at ends of cod-ends not shown). Figure courtesy of Scott Polfrey and Daniel Ashurst, British Antarctic Survey, Engineering and Technology*

At the entrance of the cod ends is a spherical valve contained within a housing (Fig S11.2). This valve is hollow with three circular holes cut into it. The rotation of this valve starts and ends sample collection. In one position, a valve is opened into the cod-end that allows organisms to swim in. In other positions, this cod-end is sealed. There are exit holes next to the spherical valve that allows

any water funnelling through the net (for instance, during downward deployment and upward recovery) to be deflected away. The two spherical valves (one in each cod-end) are rotated by a single motor which is connected to the spherical valves via motor arms.

### **Prior to deployment**

1. Motor and programming: The motor was custom supplied by Hydro-Bios Apparatebau GmbH and is based around the motor that drives their MultiNet system. To the motor, we fitted a bespoke gearing mechanism to drive two motor arms that rotate the spherical valves. The Hydro-Bios motor was programmed via a customised version of their Ocean-Lab 3 software where times were set for the motor to rotate first to move from a closed to open position and then to move from an open to closed position.
2. Cod-end preparation: The spherical valves sealed off the cod-ends prior to deployment. To avoid pressure differentials during downward deployment, it was necessary to fill the cod-ends with water prior to deployment. For the upward looking cod-end, clips could be unfastened, the cod-end detached from the device and filled with water, and then re-attached and the clips refastened. For the downward looking cod-end, it was necessary to fill the cod-end via a tap at the end of the cod-end (see Fig. SI1.1). We used seawater taken from a CTD water sample taken just prior to the MUDL deployment, at a similar depth to the intended MUDL collection depth.

### **Deployment**

The net is deployed using the same method as for a standard WP2 or Bongo net, with the net being lowered vertically over the side of the ship and then the deployment wire paid out at an approximate rate of  $0.3 \text{ m s}^{-1}$ . Once reaching its maximum designated depth, the MUDL remains there for a preset period during which time the entrances to the cod-ends open and organisms can swim in. For the present study, this collection period was set to 20 mins. The net was then recovered at a hauling-in rate of approximately  $0.3 \text{ m s}^{-1}$  and secured upright on deck.

### **Post-deployment**

The sample within the upward looking cod-end could be recovered through simply opening the tap and letting the contents gently drain into a bucket partially prefilled with filtered seawater to cushion the flow of organisms into it. For the downward looking cod-end, firstly it was necessary to untether the bottom narrow end of the net from the cod-end. A partially prefilled bucket was then held underneath the cod-end. Direct communication with the motor was established and it was instructed to rotate and unseal the cod-end, allowing the contents to flow out into the bucket.

### **Further details on the spherical valve mechanism**

The different positions of the spherical valve are illustrated in Figs. SI1.3 to Fig SI1.4, in which the outer housing has been cut away to show the valve itself. At the start of the deployment, the valve is in the closed position (Fig SI1.3). The cod-end is sealed and any water flowing through the net, as it travels downward, is deflected through the exit holes.



*Fig. SI1.3. Position during downward deployment. Cod ends are sealed, water is deflected out of exit hole (NB. Taps at ends of cod-ends not shown). Figure courtesy of Scott Polfrey and Daniel Ashurst, British Antarctic Survey, Engineering and Technology*

Once the net reaches the deployment depth, the valve rotates, which opens up a conduit from the net to the cod-end and seals the exit holes (so avoiding any individuals taking a short-cut into the cod-end; Fig SI1.4)



*Fig SI1.4. Position during sample collection. The entrance to the cod-end is now open, allowing organisms to swim in (NB. Taps at ends of cod-ends not shown). Figure courtesy of Scott Polfrey and Daniel Ashurst, British Antarctic Survey, Engineering and Technology*

At the end of a preset time (see above), the valve rotates once more, sealing off the cod-end so that it is in the same conformation as during downward deployment (Fig SI1.3). This means that any water passing through the net is deflected through the exit holes during upward recovery and the sample within the cod-ends is sealed from any contamination.

## Supplementary Information 2: Comparison of catches between MUDL net and vertically deployed mini Bongo net

Victoria Dewar-Fowler<sup>1</sup>, Carol Robinson<sup>2</sup>, Ryan A. Saunders<sup>1</sup>, Geraint A. Tarling<sup>1\*</sup>

1. British Antarctic Survey, High Cross, Madingley Rd, Cambridge, CB3 0ET, UK

2. School of Environmental Sciences, University of East Anglia, Norwich, NR4 7TJ, UK

\* corresponding author

### Rationale

To provide a context for the capture efficiency of the MUDL Net, a mini Bongo net was deployed vertically to a maximum depth of 70 m at approximately the same time as a MUDL deployment at Polar Front station PF4. We report on the total number of organisms captured by the respective nets as well as the proportional composition of different zooplankton taxonomic groups.

### Methods

The design and method deployment of the MUDL net is described in detail in the main manuscript and will not be further described here. The mini-Bongo net had an 18 cm mouth diameter with 53  $\mu\text{m}$  meshed net tapering to the cod end. Both nets were deployed at Polar Frontal Zone station PF4 (53.930°S, 49.154°W) within one hour of each other on 4/1/2017 (mini-Bongo between 21:32 and 21:37 GMT; MUDL between 21:42 and 22:20). The mini-Bongo went to a maximum depth of 70 m, the MUDL was sent to a depth of 100 m and opened for 29 mins before subsequent recovery. Both nets were within the mixed layer as defined by the temperature and salinity profiles (Fig. 3). Upon retrieval, the mini-Bongo sample was filtered and preserved in 95% ethanol. The preserved sample was sent to Morski Instytut Rybacki, Poland for zooplankton taxonomic analysis, using the following protocol: any organisms larger than 10 mm were removed from the aliquot and recorded before the sample was sorted; the aliquot was then sorted and all plankton identified to the lowest possible taxonomic level; the raw counts of each species were multiplied by the inverse of the sample fraction to give a whole sample count for each species/ stage recorded. The MUDL net samples were frozen and subsequently preserved back at the home laboratory before taxonomic identification and abundance analyses under a light microscope (see the main manuscript for full details).



## Results

We found the MUDL net to catch approximately 4.5 % and 0.3 % of the total mini Bongo catch in the downward looking and upward looking nets, respectively (Figure SI2.1). In terms of the patterns of proportional taxonomic composition of the two net types, catches were broadly similar, with cyclopoid copepods being the most abundant taxa across all samples (Figure SI2.2a). Nevertheless, certain taxa found in the mini-Bongo were absent from the MUDL, including annelids, appendicularians and tunicates. Furthermore, an ANOVA on Ranks found significant differences in the composition of the two net types ( $F_{2,26}=21.29$ ,  $P < 0.001$ ), further resolved by Dunn's pairwise tests (mini-Bongo versus downward looking MUDL:  $P < 0.001$ ; mini-Bongo versus upward looking MUDL,  $P=0.001$ ). Most notably, the proportional abundance of the dominant taxonomic groups, calanoid copepods, was significantly greater in the MUDL samples, accounting for almost 40 % and 30 % of the total catch in the downward and upward looking nets as compared to less than 20 % in the mini Bongo sample (Figure SI2.2b). There were other minor differences between net types in the proportional abundance of rare taxa such as Euphausiidae, Gastropoda and Harpacticoids, but this is as likely to be influenced by natural variation as opposed to instrumental selectivity.

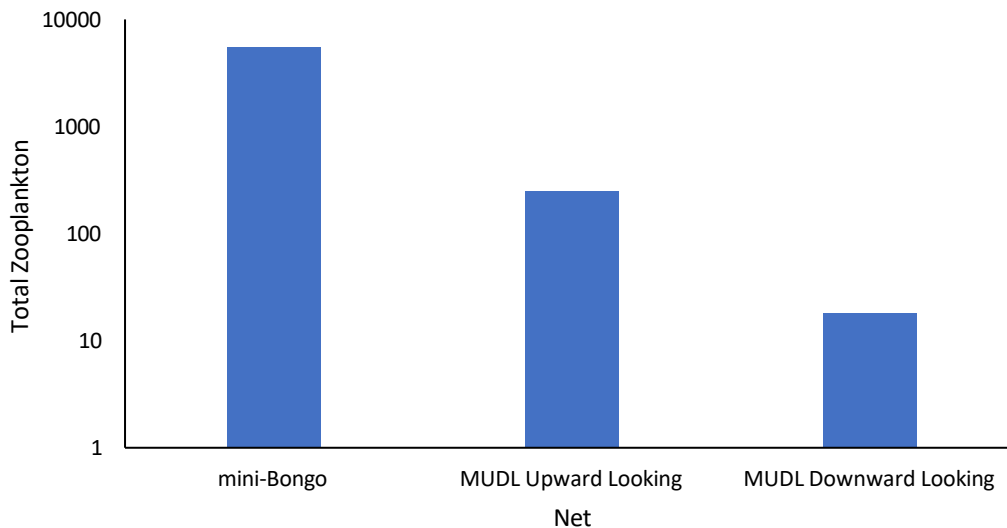


Figure SI2.1: Total number of zooplankton caught in each of the mini-Bongo, upward and downward looking nets at PF4. All nets were deployed to 100 m. mini- Bongo net was vertically hauled to the surface from 100 m, while the MUDL net only sampled whilst stationary at 100 m.

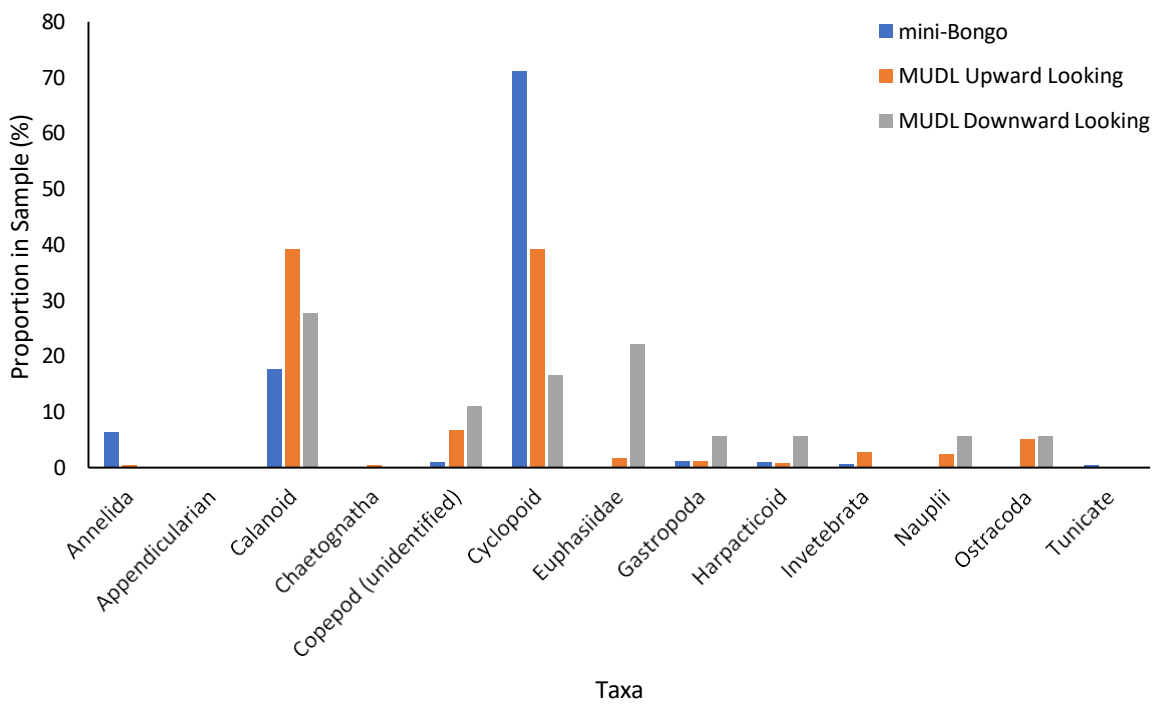
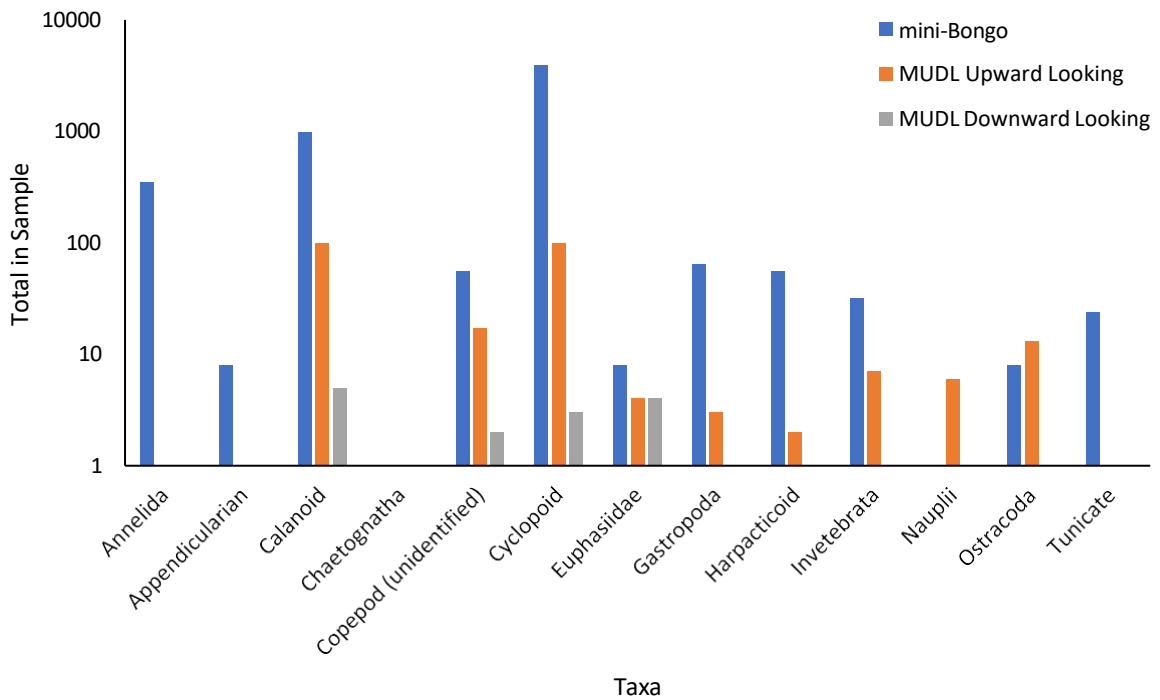


Figure SI2.2: Comparisons of MUDL and Bongo nets. (Upper) Total abundance of zooplankton in each taxa found in the mini Bongo (blue), the upward looking MUDL net (orange) and the downward looking MUDL net (grey). (Lower) Relative proportions of each zooplankton taxa found within each of the net samples for the mini Bongo (blue), the upward looking MUDL net (orange) and the downward looking MUDL net (grey).

## Conclusions

It is unsurprising that vertical integration of the water column, as performed by the mini-Bongo, will collect far more organisms per unit area compared to the MUDL into which organisms must swim in order to be captured. However, the proportional composition of different taxonomic groups was comparatively similar between the two net types. Differences between dominant taxa were found, with the MUDL more likely to catch a greater proportion of calanoid copepods and the mini-Bongo, a greater proportion of cyclopoid copepods. This may reflect the greater swimming capabilities of the calanoids, making them more likely to move into the net than the less motile cyclopoids.